Dynamic operation of distribution grids with the integration of photovoltaic systems and distribution static compensators considering network reconfiguration

Ahmed T Hachemi, Fares Sadaoui, Abdelhakim Saim, Mohamed Ebeed, Salem Arif

Energy Reports 12 (2024) 1623–1637

Contents lists available at ScienceDirect

Energy Reports

journal homepage: www.elsevier.com/locate/egyr

Research paper

Dynamic operation of distribution grids with the integration of photovoltaic systems and distribution static compensators considering network reconfiguration

Ahmed. T. Hachemi [a,d], Fares Sadaoui [a], Abdelhakim Saim [b,*], Mohamed Ebeed [c], Salem Arif [d]

[a] Electrical Engineering Laboratory, University of Kasdi Merbah Ouargla, Algeria
[b] Nantes Université, Institut de Recherche en Énergie Électrique de Nantes Atlantique, IREENA, UR 4642, Saint-Nazaire F-44600, France
[c] Department of Electrical Engineering, Faculty of Engineering, Sohag University, Sohag 82524, Egypt
[d] LACoSERE Laboratory, University of Amar Telidji, Laghouat 03000, Algeria

ARTICLE INFO

Keywords:
Renewable Energy Sources
Distribution network
Optimal operation
Horned lizard optimisation algorithm
Distribution static compensators
Network reconfiguration

ABSTRACT

The optimal operation of Distribution Networks (DNs) using network reconfiguration has become more critical in the modern power system due to the widespread use of Renewable Energy Sources (RESs) and the imbalance between load demand and energy provided by RESs. However, attaining the most efficient functioning while integrating RESs is a challenging endeavor due to the unpredictability of the electrical system and the complexities associated with network reconfiguration. Integrating Distribution Static Compensators (D-STATCOMs) with network reconfiguration is powerful for improving voltage deviation reducing overall costs, and minimizing active power losses, while successfully accommodating the fluctuating characteristics of renewable energy sources. To tackle these difficulties, we offer the Horned Lizard Optimization Algorithm (HLOA), a new approach for optimizing the operation of DNs. The efficacy of HLOA is showcased on the IEEE 33-bus DN, to minimize costs, voltage deviations, real power losses, and emissions in the presence of unpredictable factors like photovoltaic (PV) uncertainties, price changes, and load demand. The analysis encompasses three case studies: one focused on optimizing operation solely with PV integration, another using both PV and D-STATCOM integration, and a third incorporating PV, D-STATCOMs, and network reconfiguration. The results indicate that the combination of PV, D-STATCOMs, and network reconfiguration significantly decreases overall cost by 45.6 %, real power losses are reduced by 66.3 %, and voltage variations are improved by 71.04 %. Emissions are mitigated by 36.72 % compared to the base case.

1. Introduction

1.1. Motivation

The growing integration of renewable energy sources (RESs), like solar photovoltaic (PV) systems, into updated DNs brings significant economic and environmental benefits (Emrani and Berrada, 2024; Hassan et al., 2024). However, the inherent temperature and solar radiation variability make the power output from distributed generators (DGs) unpredictable, introducing new operational challenges. This variability underscores the need for probabilistic assessments to manage and mitigate network operations risks effectively (Hasanien et al., 2024; Khalid, 2024). Additionally, network reconfiguration, a strategy involving the adjustment of the distribution lines' topological structure, proves essential for improving network performance and reliability, especially with the fluctuating nature of RESs (Bahrami et al., 2024; Abbas et al., 2024). Deploying D-STATCOMs further enhances network efficiency by providing a cost-effective way to improve stability and load capacity. To maximize the benefits of D-STATCOMs, their optimal placement and sizing must be determined, considering both economic and technical aspects (Kilic et al., 2024; Kanase and Jadhav, 2024). The complexity of these decisions is increased by the stochastic nature of DNs and the interdependence of various uncertain variables. However, techniques such as Monte Carlo simulation (MCS) and the Scenario Reduction Algorithm (SRA) offer robust tools for addressing these complexities, enabling more effective and reliable network management.

* Corresponding author.
E-mail addresses: hachemi.ahmedtidjani@univ-ouargla.dz (Ahmed.T. Hachemi), sadaoui.fares@univ-ouargla.dz (F. Sadaoui), abdelhakim.saim@univ-nantes.fr (A. Saim), mebeed@eng.sohag.edu.eg (M. Ebeed), s.arif@lagh-univ.dz (S. Arif).

https://doi.org/10.1016/j.egyr.2024.07.050
Received 7 May 2024; Received in revised form 16 July 2024; Accepted 24 July 2024
Available online 31 July 2024

Acronyms

BIBC	Bus-injection to branch-current
BWO	Beluga whale optimization
DGs	Distributed generators
DNs	Distribution networks
D-STATCOMs	Distribution static compensators
HLOA	Horned lizard optimization algorithm
MCS	Monte carlo simulation
PDFs	Probability density functions
PV	Photovoltaic
RESs	Renewable energy sources
RSA	Reptile search algorithm
SCA	Sine cosine algorithm
SRA	Scenario reduction algorithm
TE	Total emission
TVD	Total voltage deviation
TRPL	Total real power losses

Symbols

C_{Grid}	Cost of electricity drawn from the grid
C_{PV}	Cost of PV
C_{Loss}	Cost of losses
$C_{DSTATCOM}$	Cost of D-STATCOMS
CO^2, NO_X, SO_2	Carbon dioxide, nitrogen oxides, and sulfur dioxide
F_1, F_2, F_3, F_4	Objective functions
$\text{Fitness}_{\min}$, $\text{Fitness}_{\max}$	Best and worst fitness values
$Fitness(i)$	Fitness value of the i^{th}search agent at this stage
$I_i, I_{Up,i}$	Current flowing through the i^{th} line, and the upper limit of current
L	Load demand
Max_iter	Maximum allowable iterations or generations
NT	Number of branches
$r1$, $r2$, $r3$, $r4$	The distinct integer values
P	Price level
$P_{(i,t)}$, $Q_{(i,t)}$	Real and reactive power flows on the branch i
$P_{Grid(t)}$	Power from the grid at each hour t
$P_{Loss,i}(t)$, $Q_{Loss,i}(t)$	Active and reactive power losses at unit i and time t
$P_{Load,i}(t)$, $Q_{Load,i}(t)$	Active and reactive power consumed by loads at unit i and time t
$P_{PV,i}(t)$	Active power from photovoltaic units at unit i and time t
$P_S(t)$, $Q_S(t)$	System's active and reactive power generation at time t
R_i	Resistance of branch i
T	Variable temperature
$Q_{DSTATCOM,i}(t)$	Reactive power provided by D-STATCOM units
$V_{s(i,t)}$	Voltage at the sending node of the branch i
$V_{(i,t)}$	Voltage at node i during the time interval t
$\vec{x}_i$	Position of a new search agent
$\vec{x}_{best}$ (t)	Position of the best performing agent from the current generation
μ	Mean
σ	Standard deviation
Γ	Gamma function
∂,τ	Shape parameters
G	Normalized solar radiation
ϑ_{Grid}	Price of grid electricity
ε_1, ε_2, ε_3, ε_4	Weights
θ	Binary indicator

1.2. Related work

The optimal operation of distribution networks has been addressed from various angles. The authors in (Ebeed et al., 2024a) utilize inverter-based PV systems with or without inherent D-STATCOM capabilities to enhance the dependability and safety of DNs, demonstrating their method's superiority on the IEEE 33-bus test network. Reactive power capabilities of PV smart inverters are explored by (Tatikayala and Dixit, 2024) as D-STATCOMs to resolve voltage control issues, integrating them with conventional devices to minimize energy dissipation. Dynamic power compensation in AC DNs using PV-D-STATCOMs is detailed in (Montoya et al., 2024), where a step-by-step approach is used to address multi-period power flow problems, highlighting the dual functionality of PV-D-STATCOMs as both PV production plants and reactive power compensators. The study in (Woldesemayat et al., 2024) focuses on electricity distribution losses in Gesuba town's 15 kV system, identifying the high loss factor and limited voltage stability while determining the optimal bus size and location of D-STATCOM for improved performance. Innovative charging and battery swapping station integration into radial distribution systems using renewable DGs and D-STATCOM is introduced in (Balu and Mukherjee, 2024), effectively mitigating demand issues from EV charging and swapping stations based on student psychology optimization. With the rise of electric vehicles, (Yuvaraj et al., 2023) discusses the challenges to distribution systems due to increased electricity demand, proposing a method using the Slime Mould Algorithm to optimize the placement and sizing of components in radial distribution systems. The utilization of photovoltaic sources and D-STATCOM devices to reduce annual grid operating expenses over 20 years is explored in (Rincón-Miranda et al., 2023). A probabilistic mixed-integer convex model for optimizing locations and sizes of D-STATCOMs in electrical networks, considering renewable energy integration and demand fluctuations, is presented by (Gil-González, 2023), aiming to minimize annual installation and operation costs. The research in (Marquez et al., 2023) proposes a cost-effective strategy for improving distribution system efficiency through tie-line network reconfiguration and distributed energy resources, calculating the optimum Energy Not Supplied index. In (Hachemi et al., 2023a), the authors present the Modified Reptile Search Algorithm, this technique aims to improve network performance by reducing costs, voltage variations, and system instability, thereby enhancing overall system stability. The Multi-Group Flight Slime Mould Algorithm, a flexible reconfiguration approach for IEEE-33 and IEEE-118 bus DNs that models dynamic reconfiguration across multiple periods, is introduced in (Pan et al., 2022), enhancing economic efficiency and operational safety. The efficacy of Demand Side Response and renewable energy integration in the IEEE 118-bus distribution system is showcased in (Hachemi et al., 2023b), introducing the Improved Walrus Algorithm to optimize costs and enhance stability amid fluctuating conditions. In (Noruzi Azghandi et al., 2023), the authors suggest adjusting the distribution network to better accommodate distributed generation units and electric vehicles. This method considers various factors, including energy loss, operational expense, and unsupplied energy. In (Ramadan et al., 2022), the authors introduce a highly effective method for optimizing the size and location of renewable distributed generators in radial distribution systems, addressing the inherent uncertainties in the power system. The approach employs an MCS technique alongside an Artificial Gorilla Troops Optimizer. The integration of PV systems into DNs on a large scale using a county-wide promotion model and the Improved Multi-Objective Teaching-Learning Optimization algorithm is elaborated in (Liu et al., 2024), achieving optimal integration of distributed PV systems and enhancing voltage profiles. The multi-objective hierarchical model for optimal distributed generation

planning that enhances power reliability and efficiency while reducing annual costs and energy losses is presented in (Li et al., 2024). In (Mahdavi et al., 2022), the authors examine the influence of load patterns on switching sequences in three distribution systems,the objective is to assess the significance of load profiles in reducing energy losses wirth network reconfiguration. The study in (Liao et al., 2023), presents a method for dynamically reconfiguring hybrid distribution networks, this approach considers the cost of aging cycles and demand response, and is based on non-ideal battery energy storage models. In (Wang et al., 2021), the authors presents a thorough examination of operation scenarios to achieve the most efficient distribution network reconfiguration, the system employs the K-Means technique for clustering common cases and utilizes time interval loss index to assess the overall network loss performance. The authors in (Amigue et al., 2021), proposed a method to identify the most optimal location for integrating PVs into the energy grid, this algorithm aims to minimize power losses and improve the voltage profile. The study in (Ortega-Romero et al., 2023), suggests a methodology for determining where distributed generation units should be placed in a lengthy, medium-voltage electrical network to minimize energy losses, raise voltage levels, and improve system reliability.In the context of our discussion on related work, we conducted a detailed comparison of all previously mentioned studies to explore the scientific gaps that our current research aims to address in Table 1.

1.3. Research gaps

The research gaps identified in these studies are outlined below:

1. Many studies (Kanase and Jadhav, 2024; Ebeed et al., 2024a; Tatikayala and Dixit, 2024; Montoya et al., 2024; Woldesemayat et al., 2024; Balu and Mukherjee, 2024; Yuvaraj et al., 2023; Rincón-Miranda et al., 2023; Gil-González, 2023; Hachemi et al., 2023a, 2023b; Noruzi Azghandi et al., 2023; Ramadan et al., 2022; Liu et al., 2024; Li et al., 2024; Mahdavi et al., 2022; Liao et al., 2023; Wang et al., 2021; Amigue et al., 2021; Ortega-Romero et al., 2023) do not consider relevant uncertainties related to energy prices, load behavior, and weather conditions. This limits the ability to develop robust and reliable solutions that can adapt to varying conditions in power distribution systems.
2. Reconfiguration is not addressed in several studies (Kanase and Jadhav, 2024; Ebeed et al., 2024a; Tatikayala and Dixit, 2024; Montoya et al., 2024; Woldesemayat et al., 2024; Balu and Mukherjee, 2024; Yuvaraj et al., 2023; Rincón-Miranda et al., 2023; Marquez et al., 2023; Pan et al., 2022; Noruzi Azghandi et al., 2023; Ramadan et al., 2022; Liu et al., 2024; Li et al., 2024; Amigue et al., 2021; Ortega-Romero et al., 2023). This limits the optimization potential and adaptability of the power distribution systems.
3. References (Kanase and Jadhav, 2024; Ebeed et al., 2024a; Tatikayala and Dixit, 2024; Montoya et al., 2024; Woldesemayat et al., 2024; Balu and Mukherjee, 2024; Yuvaraj et al., 2023; Rincón-Miranda et al., 2023; Gil-González, 2023; Marquez et al., 2023; Hachemi et al., 2023a; Pan et al., 2022; Hachemi et al., 2023b; Noruzi Azghandi et al., 2023; Liu et al., 2024; Li et al., 2024; Mahdavi et al., 2022; Liao et al., 2023; Wang et al., 2021; Amigue et al., 2021; Ortega-Romero et al., 2023) focus only on single or dual objectives, either technical or economic, and often neglect environmental objectives. Only study (Ramadan et al., 2022) attempts a more comprehensive approach by considering multiple objectives. However, this study has limitations, such as not accounting for all uncertainties within the system and not addressing the reconfiguration of the system.

Based on these gaps, an essential question is how network reconfiguration, combined with the integration of Photovoltaic Systems and Distribution Static Compensators, will influence the dynamic operation of distribution grids in the presence of uncertainties related to price, loading, temperature, and irradiance.

1.4. Novelty and contribution

1. The main novel contributions of this study work, aimed at addressing the aforementioned research gaps, are visually illustrated in Fig. 1 and outlined below:
2. A techno economic and environmental investigation is presented for optimal integration of PV system and D-STATCOM along with reconfiguration of distribution systems.

Table 1
Comparative analysis between the current study and previous literature.

Reference	Systems		Uncertainty				Reconfiguration	Objective Functions		
	PV	D-STATCOM	Price	Loading	Temperature	Irradiance		Technical	Economical	Environmental
(Ebeed et al., 2024a)	✓	✓	×	✓	×	✓	×	✓	×	×
(Tatikayala and Dixit, 2024)	✓	✓	×	×	×	×	×	✓	×	×
(Montoya et al., 2024)	✓	✓	×	×	×	×	×	✓	✓	×
(Woldesemayat et al., 2024)	×	✓	×	×	×	×	×	✓	×	×
(Balu and Mukherjee, 2024)	✓	✓	×	✓	×	✓	×	✓	✓	×
(Yuvaraj et al., 2023)	✓	✓	×	×	×	×	×	✓	×	×
(Rincón-Miranda et al., 2023)	✓	✓	×	×	×	×	×	×	✓	×
(Gil-González, 2023)	×	✓	×	×	×	×	×	×	✓	×
(Marquez et al., 2023)	✓	×	×	×	×	×	✓	✓	✓	×
(Hachemi et al., 2023a)	✓	×	✓	✓	✓	✓	×	✓	✓	×
(Pan et al., 2022)	×	×	×	×	×	×	✓	✓	✓	×
(Hachemi et al., 2023b)	✓	×	✓	✓	✓	✓	×	✓	✓	×
(Noruzi Azghandi et al., 2023)	✓	×	×	×	×	×	✓	✓	✓	×
(Ramadan et al., 2022)	✓	×	✓	✓	×	✓	×	✓	✓	✓
(Liu et al., 2024)	×	×	×	×	×	×	×	✓	×	×
(Li et al., 2024)	✓	×	×	✓	×	✓	×	✓	✓	×
(Mahdavi et al., 2022)	×	×	×	×	×	×	✓	×	✓	×
(Liao et al., 2023)	✓	×	×	×	×	×	✓	×	✓	×
(Wang et al., 2021)	×	×	×	×	×	×	✓	✓	×	×
(Amigue et al., 2021)	✓	×	×	×	×	×	×	✓	×	×
(Ortega-Romero et al., 2023)	✓	×	×	×	×	×	×	✓	×	×
This paper	✓	✓	✓	✓	✓	✓	✓	✓	✓	✓

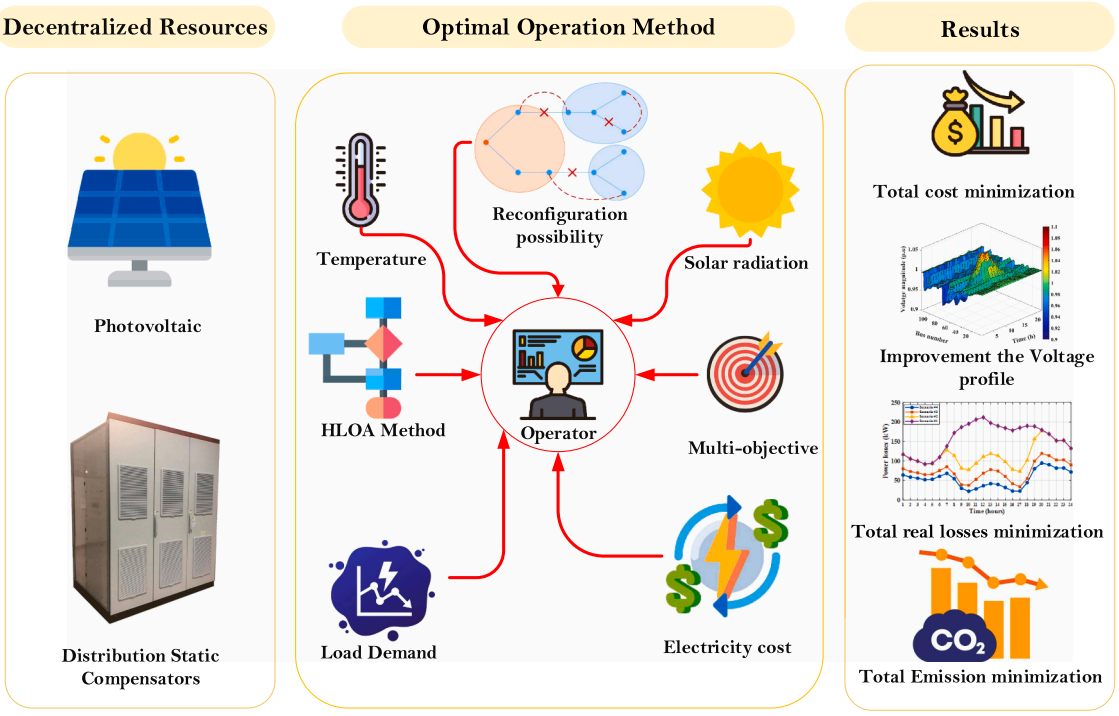

Fig. 1. The summary of the proposed framework.

3. Exploring the synergies between PV system, D-STATCOMs, and network reconfiguration to optimize the alignment of renewable generation with flexible demand.
4. Utilizing the probability density functions and the Scenario Reduction Algorithm (SRA) along with Monte Carlo simulation (MCS) for handling the uncertainties of the load power, price fluctuations, and the yielded power from the PV system.
5. A novel HLOA algorithm is proposed for the first time to allocate the PV system and D-STATCOM for optimizing four objective functions simultaneously including the cost, the emissions, the voltage profile, and real power losses of the distribution system.
6. A comprehensive comparison between the suggested HLOA technique and Reptile Search Algorithm (RSA), the Sine Cosine Algorithm (SCA), and the Beluga Whale Optimization (BWO) to demonstrate the effectiveness of HLOA.

This work is useful for society and practitioners as it provides innovative solutions for integrating renewable energy sources into existing grids, enhancing the efficiency and sustainability of energy distribution systems.

1.5. Organization of the article

This paper is organized as follows: Section 2 addresses uncertainties related to temperature, solar radiation, pricing, and load demand. Section 3 outlines the problem formulation for the electrical distribution network aimed at improving operational costs, voltage stability, power loss, and emissions. This provides the foundation for applying the proposed HLOA algorithm, detailed in Section 4. Section 5 discusses the simulation results and analysis. The document concludes with Section 6, summarizing the study's findings and the implications of the results.

2. Probabilistic uncertainties

This study delves into the uncertainties of four critical variables: temperature, solar radiation, pricing, and load demand. Understanding these uncertainties is crucial as it allows for better risk assessment and strategic planning in energy systems management. To model the system's uncertainties, the mean (μ) and the standard deviation (σ) values are derived from meteorological data and the variations in loads and prices. Table 2 lists the μ and σ values for temperature, solar radiation, pricing, and load demand over 24 h, providing a foundation for understanding and managing the risks associated with these fluctuations in the energy system.

2.1. Temperature probabilistic presentation

In the probabilistic analysis of temperature uncertainties, the variability is expressed through the normal distribution, as outlined in the following equation (Hachemi et al., 2023b):

$$f(T) = \frac{1}{\sigma_T\sqrt{2\pi}}\exp\left[-\frac{(T - \mu_T)^2}{2{\sigma_T}^2}\right] \quad (1)$$

Where μ_T represents the mean temperature, σ_T is the standard deviation indicating the spread around the mean, and T is the variable temperature. This model efficiently quantifies the statistical distribution of temperature fluctuations.

2.2. Solar radiation probabilistic presentation

In the study of solar radiation, its variability can also be modeled probabilistically. The distribution of solar radiation is mathematically represented using the Beta distribution, detailed by the equation (Piri et al., 2023; Akbari et al., 2017):

$$f(G) = \begin{cases} \frac{\Gamma(\partial+\tau)}{\Gamma(\partial)\Gamma(\tau)} s^{(\partial-1)}(1-G)^{(\tau-1)} & 0 \le G \le 1; \partial, \tau \ge 0 \\ 0 & \text{otherwise} \end{cases} \quad (2)$$

Where Γ denotes the gamma function, ∂ and τ are shape parameters that influence the form of the distribution, and G represents the normalized solar radiation. This approach allows for a nuanced description of the fluctuations in solar energy availability.

Table 2
The μ and σ values of the uncertain parameters.

Hour	Temperature		Solar Radiation		Price		Load Demand	
	μ	σ	μ	σ	μ	σ	μ	σ
1	17.174	7.3267	0	0	0.11	0.0275	76.19	8.28
2	16.5741	7.2526	0	0	0.1	0.025	72.13	8.49
3	16.0557	7.1976	0	0	0.11	0.0275	70.26	8.29
4	15.5933	7.1503	0	0	0.09	0.0225	68.04	8.21
5	15.1806	7.0987	0	0	0.11	0.0275	68.6	8.56
6	15.45	7.6149	0	0	0.11	0.0275	73.66	10.15
7	17.393	8.4126	22.1314	0.028833	0.13	0.0325	82.2	13.25
8	20.4664	8.6512	134.9197	0.100448	0.15	0.0375	90.56	15.11
9	23.5787	8.6734	335.1481	0.133864	0.26	0.065	94.59	14.26
10	26.0153	8.2898	543.2130	0.145496	0.3	0.075	96.52	12.81
11	27.7378	7.9859	716.3761	0.151267	0.35	0.0875	98.43	12
12	28.9056	7.7783	834.0451	0.156275	0.4	0.1	100	11.47
13	29.5949	7.6528	887.6853	0.159055	0.4	0.1	96.68	11.65
14	29.8343	7.5974	867.7212	0.160291	0.5	0.125	95.34	12.37
15	29.6227	7.6125	779.3058	0.158523	0.3	0.075	93.85	12.9
16	28.7845	7.8703	630.9906	0.154956	0.3	0.075	92.98	13.14
17	26.6448	8.669	436.3135	0.14444	0.4	0.1	93.29	13.87
18	24.021	8.241	224.0758	0.123348	0.5	0.125	94.91	14.7
19	22.4503	7.7399	62.2966	0.063725	0.3	0.075	95.23	14.31
20	21.4333	7.7191	3.2811	0.005689	0.26	0.065	93.6	12.73
21	20.4501	7.6865	0	0	0.15	0.0375	90.48	10.36
22	19.5017	7.622	0	0	0.13	0.0325	86.01	8.63
23	18.6408	7.5313	0	0	0.1	0.025	86.19	9.03
24	17.8621	7.4262	0	0	0.11	0.0275	80.35	8.75

In the probabilistic model for solar radiation, the Beta distribution parameters τ and ∂ are determined based on the mean μ and variance σ^2 of the distribution. The parameter τ is defined by the equation (Ebeed et al., 2020):

$$\tau = (1-\mu) \times \left(\frac{\mu \times (1+\mu)}{\sigma^2} - 1 \right) \tag{3}$$

This parameter adjusts to reflect the skewness of the distribution towards lower values. Meanwhile, the parameter ∂ is calculated with (Zubo et al., 2018):

$$\partial = \frac{\mu \times \tau}{1-\mu} \tag{4}$$

The real power output of the PV units can be calculated using the formula below (Diaf et al., 2007).

$$T_c(t) = T_a(t) + \frac{G(t)}{800} \times (NOCT - 20) \tag{5}$$

$$P_{PV}(h) = A_{PV} \times \eta_{PV}(t) \times G(t) \tag{6}$$

In which

$$\eta_{PV}(t) = \&\eta_r \times \eta_t \times \left[1 - \gamma \times (T_a(t) - T_r) - \gamma \times G(t) \times \left(\frac{NOCT - 20}{800} \right) \right] \&$$

(7)

A_{PV}, is the area covered by the PV panel in square meters; T_c and T_a, which represents the cell temperature and ambient temperature respectively; G, standing for solar irradiance; $NOCT$, the Nominal Operating Cell Temperature; γ, known as the temperature coefficient; and η_r along with η_{PV}, referring to the reflection efficiency and the direct efficiency of the PV array, respectively.

2.3. Price probabilistic presentation

In the probabilistic representation of price data, the normal probability density function is employed to quantify the distribution of price fluctuations around a mean value. This is mathematically described by the function $f(P)$, which is given by (Morstyn et al., 2019; Shojaabadi et al., 2016):

$$f(P) = \frac{1}{\sigma_P \sqrt{2\pi}} \exp\left[-\frac{(P - \mu_P)^2}{2{\sigma_P}^2} \right] \tag{8}$$

In this formula, μ_P is the mean price, and σ_P is the standard deviation, indicating the spread of price values around the mean, the variable P represents the price level.

2.4. Load Demand probabilistic presentation

The probability distribution of load demand L is captured through the normal probability density function $f(L)$, which delineates how the demand values are spread around the mean. This function is defined as (Zubo et al., 2018; Kamel et al., 2024):

$$f(L) = \frac{1}{\sigma_L \sqrt{2\pi}} \times \exp\left[-\frac{(L - \mu_L)^2}{2\sigma_L^2} \right] \tag{9}$$

Within this expression, μ_L signifies the average load demand, serving as the central point around which load values are expected to fluctuate, while σ_L denotes the standard deviation, providing a measure of the spread or variability of the load demand around the mean.

The entire process of establishing parameters for the PDF is based on the collected data (Rubinstein and Kroese, 1981; Ebeed et al., 2024b). This data establishes parameters for variables, including temperature, solar irradiation, load, and pricing. Monte Carlo simulations are employed to generate 1000 data points for these variables. However, the significant computational demand arising from the vast number of potential scenarios necessitates a more streamlined approach. To mitigate this, the Scenario Reduction Algorithm (SRA) is implemented, effectively reducing the total number of scenarios to 25 (Growe-Kuska et al., 2003; Biswas et al., 2019).

Fig. 2 presents a comprehensive distribution of scenarios derived from MCS across various parameters critical to energy system analysis. These scenarios help in understanding the probabilistic nature of these variables.

The way SRA is represented is as follows:

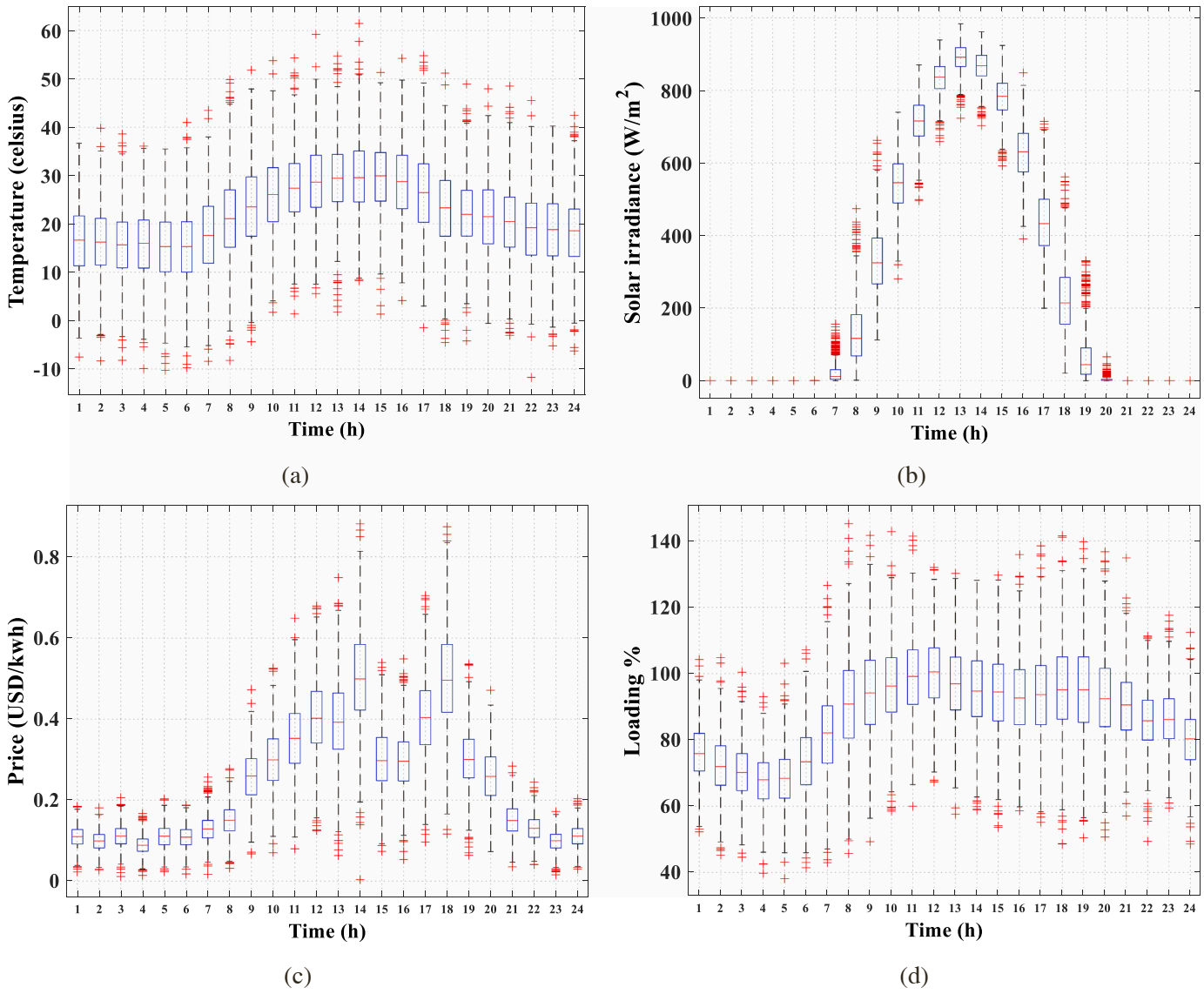

Fig. 2. Monte Carlo simulation scenario distribution for (a) Temperature, (b) Solar Irradiance, (c) Pricing, and (d) Load Demand.

1. Initialize N_0 scenarios, represented by vectors Y_i for i=1, 2, …, N_0 . N_0 represent the scenario generated by MCS.
2. Assign an equal probability to each scenario: $\Delta_0 = \frac{1}{N_0}$
3. Compute distance between each pair of scenarios by calculating the norm.
4. Distance between scenarios Y_i and Y_j is $d_{ij} = \|Y_i - Y_j\| \, \|Y_i - Y_j\|$.
5. Calculate the distances between all pairs of scenarios (distance matrix D).
6. Set N_{Dy} to N_0 and define the target number of scenarios N_{SC}.
7. Identify the smallest non-zero distance in the distance matrix D
8. Determine the two scenarios m and n corresponding to this minimum distance.
9. Compare the probabilities Δ_m and Δ_n
10. If $\Delta_m \geq \Delta_n$, eliminate scenario n and update Δ_m by adding Δ_n.
11. Otherwise, eliminate scenario m and update Δ_n by adding Δ_m.
12. Modify the distance matrix D by removing the row and column of the eliminated scenario.
13. Decrement N_{Dy} by 1.
14. Check if N_{Dy} equals N_{SC} (If N_{Dy} equals N_{SC}, terminate the algorithm; otherwise, repeat the reduction loop).

Fig. 3 illustrates the results of the SRA applied to MCS results for various key parameters. This reduction is crucial for simplifying the complexity of the problem while maintaining the integrity of the data's variability.

3. Problem formulation

This section explores the formulation of key performance indicators for optimizing a power distribution system. The focus includes Total Real Power Losses (*TRPL*), which asses system efficiency, Total Operation Cost (*C*), which calculates the comprehensive costs of running the network, Total Voltage Deviation (*TVD*) for network stability, and Total Emission (*TE*) reflecting the environmental impact. Each parameter is calculated using specific formulas to guide strategies for reducing costs, emissions, and improving system reliability and efficiency.

3.1. Objective functions

3.1.1. Total real power losses

Reducing Total Real Power Losses (TRPL) is important as it directly impacts the efficiency and economic operation of the power distribution system, aligning with our goal to enhance network performance and reduce operational costs. TRPL can be represented using the following

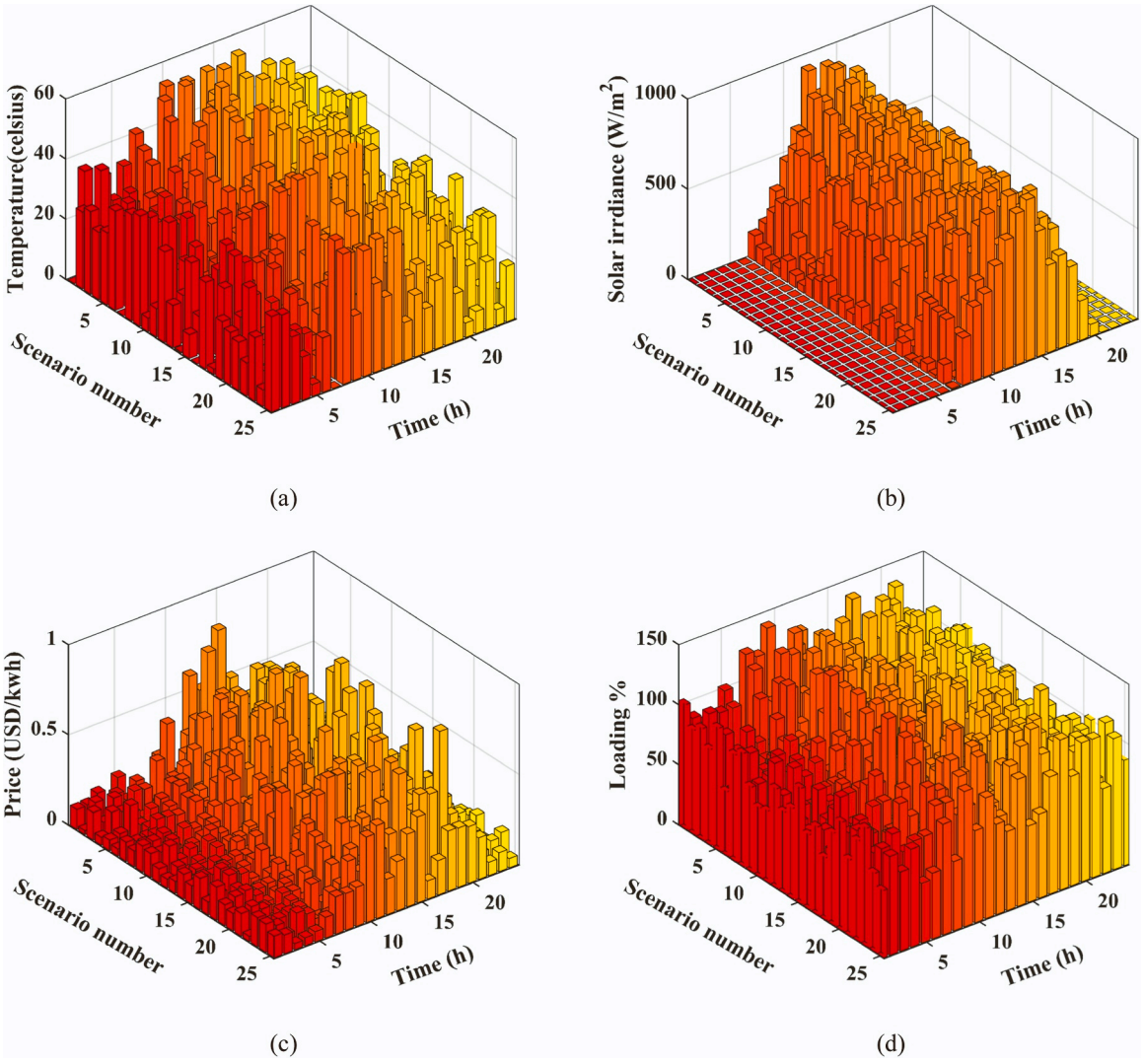

Fig. 3. Scenario Reduction Algorithm for (a) Temperature, (b) Solar Irradiance, (c) Pricing, and (d) Load Demand.

equation (Hachimi et al., 2022; Badrudeen et al., 2024):

$$TRPL = \sum_{t=1}^{24} \sum_{i=1}^{NT} P_{Loss(i,t)} \tag{10}$$

$$P_{Loss(i,t)} = \left|I_{(i,h)}\right|^2 \quad R_i = \left(\frac{P_{(i,t)}^2 + Q_{(i,t)}^2}{\left|V_{s(i,h)}\right|^2}\right) R_i \tag{11}$$

where $I_{(i,t)}$ is the current on the branch i, R_i is the resistance of branch i, $P_{(i,t)}$ and $Q_{(i,t)}$ are the real and reactive power flows on the branch i, respectively, and $V_{s(i,t)}$ is the voltage at the sending node of the branch i, $NT$is the number of branches.

3.1.2. Total operation cost

The total operation cost for a distribution network is determined by Eq. (12), which summarizes the key components of operational expenses. These include the cost of PV(C_{PV}), the cost of electricity drawn from the grid (C_{Grid}), losses incurred within the system (C_{Loss}), and the cost associated with the D-STATCOMS ($C_{DSTATCOM}$). Minimizing this aggregate cost is crucial for ensuring efficient and cost-effective operation of the power system.

$$C = C_{Grid} + \quad C_{Loss} \quad + C_{PV} \quad + C_{DSTATCOM} \tag{12}$$

In which,

$$C_{Grid} = \quad 365 \times \sum_{t=1}^{24} P_{Grid(t)} \times \vartheta_{Grid(t)} \tag{13}$$

$P_{Grid(t)}$ represents the power from the grid at each hour t, and $\vartheta_{Grid(t)}$ denotes the price of grid electricity at that hour. These factors are used to calculate the hourly cost of grid electricity, which is then summed up for all 24 h of the day and multiplied by 365 to represent the annual cost of electricity drawn from the grid.

$$C_{Loss} = 365 \times \varepsilon_{Loss} \times \sum_{t=1}^{24} P_{T\_Loss(t)} \tag{14}$$

Where ε_{Loss} is the cost per kilowatt-hour of power losses, set at 0.06 USD/kWh (Sultana and Roy, 2014). $P_{T\_Loss(t)}$ represents the power losses at each hour t over a 24-hour period.

$$C_{PV} = \quad C_{PV}^{inst} + C_{PV}^{O\&M} \tag{15}$$

Where C_{PV}^{inst} represents the installation costs associated with the PV system, and $C_{PV}^{O\&M}$ refers to the ongoing operations and maintenance costs of the PV system.

$$C_{PV}^{O\&M} = 365 \times \mu_{PV}^{O\&M} \times \sum_{t=1}^{24} \sum_{i=1}^{N_{PV}} P_{PV(i,t)} \tag{16}$$

$$C_{PV}^{inst.} = CF \times U_{PV} \times \sum_{i=1}^{N_{PV}} P_{rated\_PV(i)} \tag{17}$$

Where $\mu_{PV}^{O\&M}$ is the cost per kilowatt-hour for operations and maintenance, valued at 0.01 USD/kWh (Gampa and Das, 2015). and $P_{PV(i,t)}$ represents the power output from the i^{th} photovoltaic unit at time t. N_{PV} represents the number of photovoltaic units. For the installation costs, CF denotes the capital recovery factor, U_{PV} is the unit cost per rated power, set at 770 USD/kW, and $P_{rated\_PV(i)}$ is the rated power of the i^{th} PV system (Augustine et al., 2012).

The capital recovery factor is represented by the following equation:

$$CF = \frac{ir \times (1+ir)^N}{(1+ir)^N - 1} \tag{18}$$

Where ir represents the interest rate, and N denotes the number of periods over which the investment is amortized.

$$C_{DSTATCOM} = C_S \times Q_S \times \frac{(1+\mathfrak{q})^{Ns} \times \mathfrak{q}}{(1+\mathfrak{q})^{Ns} - 1} \tag{19}$$

Where Q_S represents the rated kVar of the D-STATCOM, C_S stands for the capital cost, Ns denotes the DSTATCOM's lifetime in years, and $\mathfrak{q}$ represents the asset rate of return (Oda et al., 2021).

3.1.3. Total voltage deviation

Reducing voltage deviation is crucial for enhancing the performance of electrical networks, particularly in stabilizing network voltage levels. This is quantified by the Total Voltage Deviation (TVD), which is given by the following equation (Asaad et al., 2023; Purlu and Turkay, 2022; Ahmed et al., 2024):

$$TVD = \sum_{t=1}^{24} \sum_{i=1}^{NB} \left| \left(V_{(i,t)} - 1\right) \right| \tag{20}$$

Where NB represents the total number of buses or nodes in the network, and $V_{(i,t)}$ denotes the voltage at node i at time t.

3.1.4. Total emission

Reducing Total Emission (TE) is crucial in our study as it directly relates to environmental sustainability and compliance with regulatory standards for air quality. The primary pollutants involved in this calculation are carbon dioxide (CO_2), nitrogen oxides (NO_x), and sulfur dioxide (SO_2), which are critical contributors to atmospheric pollution. These emissions are particularly significant in the context of power generation from grid-supplied electricity. Total Emission is represented by the following equation, with emissions measured in kilograms (kg) (Esmaeili et al., 2016).

$$TE = 365 \times \sum_{t=1}^{24} P_{Grid(t)} \times \left(CO_2^{\text{Grid}} + NO_x^{\text{Grid}} + SO_2^{\text{Grid}}\right) \tag{21}$$

Where the emissions factors for CO_2 are 921.25 kg/MWh, for NO_x are 2.2952 kg/MWh, and for SO_2 are 3.5834 kg/MWh.

In this study, the weighted penalty summation method was used to solve the multi-objective problem. This method involves combining the individual objective functions into a single aggregated objective function by assigning a weight to each objective, as described below:

$$\min(MOF) = \min(\varepsilon_1 F_1 + \varepsilon_2 F_2 + \varepsilon_3 F_3 + \varepsilon_4 F_4) \tag{22}$$

$$F_1 = \frac{TRPL_{after}}{TRPL_{befor}} \tag{23}$$

$$F_2 = \frac{C_{after}}{C_{befor}} \tag{24}$$

$$F_3 = \frac{TVD_{after}}{TVD_{befor}} \tag{25}$$

$$F_4 = \frac{TE_{after}}{TE_{befor}} \tag{26}$$

Where the terms *befor* and *after* refer to the values of parameters before and after the implementation of improvements, respectively. Additionally, the weights ε_1, ε_2, ε_3, ε_4 are all set to 0.25, equally distributing the importance across all objective functions F_1, F_2, F_3, F_4.

3.2. The system constraints

In the context of improving distribution electrical networks, it is crucial to adhere to a set of constraints that form an integral part of the design and enhancement process. These constraints ensure that the implemented improvements not only enhance performance but also comply with technical, safety, and regulatory standards.

3.2.1. Equality constraints

In the equations mentioned, the following elements are used to balance generation and consumption within the electrical distribution system (Elseify et al., 2024; Mohamed et al., 2024):

$$P_S(t) + \sum_{i=1}^{N_{PV}} P_{PV,i}(t) = \sum_{i=1}^{NT} P_{Loss,i}(t) + \sum_{i=1}^{NB} P_{Load,i}(t) \tag{27}$$

$$Q_S(t) + \sum_{i=1}^{NQ} Q_{DSTATCOM,i}(t) = \sum_{i=1}^{NT} Q_{Loss,i}(t) + \sum_{i=1}^{NB} Q_{Load,i}(t) \tag{28}$$

Where $P_S(t)$ and $Q_S(t)$ represent the system's active and reactive power generation at time t, respectively. $P_{PV,i}(t)$ denotes the active power from photovoltaic units at unit i and time t, while $Q_{DSTATCOM,i}(t)$ indicates the reactive power provided by D-STATCOM units at the same points. $P_{Loss,i}(t)$ and $Q_{Loss,i}(t)$ refer to active and reactive power losses at unit i and time t. Finally, $P_{Load,i}(t)$ and $Q_{Load,i}(t)$ account for the active and reactive power consumed by loads at unit i and time t.

3.2.2. Inequality constraints

3.2.2.1. constraints of voltage

$$V_{Lp} \le V_{(i,t)} \le V_{Up} \tag{29}$$

In the voltage constraints equation, $V_{(i,t)}$ denotes the voltage at node i during the time interval t. The permissible voltage limits are defined as V_{Lp} at 0.90 p.u. (per unit) for the lower limit and V_{Up} at 1.05 p.u. for the upper limit, ensuring that voltage levels at each node remain within a stable and safe operating range.

3.2.2.2. Constraint on the line capacity

$$I_i \le I_{Up,i} \tag{30}$$

In the constraint on line capacity, I_i represents the current flowing through the i^{th} line, and $I_{Up,i}$ denotes the upper limit of current that this particular line can safely carry.

3.2.2.3. PV and DSTATCOM constraints

$$\sum_{i=1}^{N_{PV}} P_{PV\_rated,i} \le \sum_{i=1}^{NB} P_{Load,i} \tag{31}$$

$$\sum_{i=1}^{NQ} Q_{DSTATCOM,i} \le \sum_{i=1}^{NB} Q_{Load,i} \tag{32}$$

The constraints for PV systems and D-STATCOM ensure that the

installed capacities are within safe operational limits relative to the load demand. Specifically, the total rated power output of all PV installations, denoted by $\sum_{i=1}^{NP} P_{PV\_rated,i}$, must not exceed the total power load across all nodes, $\sum_{i=1}^{NB} P_{Load,i}$. Similarly, the total reactive power compensation provided by all $\sum_{i=1}^{NQ} Q_{DSTATCOM,i}$, should not surpass the total reactive power demand of the loads, $\sum_{i=1}^{NB} Q_{Load,i}$. These constraints ensure that the PV and D-STATCOM systems are sized appropriately to support but not exceed the load requirements of the network.

3.2.2.4. Constraint of Radial Configuration. In the reconfiguration of electrical DNs, maintaining a radial configuration of the system is a crucial constraint to ensure continuity and safety in operation. A radial configuration prevents the formation of closed loops, which could lead to disturbances in electrical flow and stability issues (Şeker et al., 2021).

3.2.2.5. Constraint of Isolation. This constraint ensures that all nodes or buses in the network are active and energized post-reconfiguration (Şeker et al., 2021).

4. Horned lizard optimization algorithm (HLOA)

The Horned Lizard Optimization Algorithm (HLOA) mathematically models five defensive behaviours of the horned lizard (Peraza-Vázquez et al., 2024):

4.1. Behavior of crypsis

Crypsis is a defensive adaptation in which an organism mimics its surroundings by copying features such as color and texture or becoming nearly transparent. This allows it to blend seamlessly into its environment, making it difficult for predators or prey to detect or recognize. Such camouflage enhances an organism's ability to evade detection, significantly increasing its chances of survival in the wild. The lizard's color-changing ability to blend in with its surroundings is modelled using the CIE Lab colour space and the equation:

$$\vec{x}_i(t+1)\& = \vec{x}_{\text{best}}(t) + \left(\partial - \frac{\partial \cdot t}{\text{Max\_iter}}\right) \& \left[c_1(\sin(\vec{x}_{r_1}(t)) - \cos(\vec{x}_{r_2}(t))) - (-1)^{\theta} c_2(\cos(\vec{x}_{r_3}(t)) - \sin(\vec{x}_{r_4}(t)))\right] \tag{33}$$

In the revised formula, the position of a new search agent (symbolized as a horned lizard) for the next generation $(t+1)$ is denoted as $\vec{x}_i(t+1)$. It is determined based on the position of the best performing agent from the current generation, noted as $\vec{x}_{best}(t)$. The parameters $r1$, $r2$, $r3$, and $r4$ represent distinct integer values randomly chosen between 1 and the maximum number of agents, ensuring that $r1, r2, r3$, and $r4$ are all different. The positions of these randomly selected agents in the current generation are indicated by $\vec{x}_{r_1}(t)$, $\vec{x}_{r_2}(t)$, $\vec{x}_{r_3}(t)$, and $\vec{x}_{r_4}(t)$ respectively. The term *Max_iter* stands for the maximum allowable iterations or generations, while θ is a binary indicator. The variable ∂ is fixed at a value of 2. Furthermore, c_1 and c_2 are distinct random numbers sourced from (Peraza-Vázquez et al., 2024), which lists a normalized range of colours.

4.2. Skin darkening/lightening

Based on the need to either increase or decrease its solar thermal gain, the horned lizard can adjust its skin color by either lightening or darkening it. These changes in the lizard's skin hue are captured by Eqs. (34) and (35). Eq. (34) describes the process of lightening the skin, while Eq. (35) outlines the skin darkening method.

$$\vec{x}_{\text{worst}}(t) = \vec{x}_{\text{best}}(t) + \frac{1}{2}\text{Light}_1 \sin(\vec{x}_{r_1}(t) - \vec{x}_{r_2}(t)) \& -(-1)^{\theta}\frac{1}{2}\text{Light}_2 \sin(\vec{x}_{r_3}(t) - \vec{x}_{r_4}(t)) \& \tag{34}$$

$$\vec{x}_{\text{worst}}(t) = \vec{x}_{\text{best}}(t) + \frac{1}{2}Dark_1 \sin(\vec{x}_{r_1}(t) - \vec{x}_{r_2}(t)) -(-1)^{\theta}\frac{1}{2}Dark_2 \sin(\vec{x}_{r_3}(t) - \vec{x}_{r_4}(t)) \tag{35}$$

$Light_1$ and $Light_2$ are random integers calculated within the range from $Lightening_1$ (0 value) to $Lightening_2$ (0.4046661 value), based on normalized values from (Peraza-Vázquez et al., 2024). Similarly, $Dark_1$ and $Dark_2$ are derived between $Darkening_1$ 1 (0.5440510 value) and $Darkening_2$ (1 value), using the same table for normalization.

4.3. Blood-squirting

The Horned lizard has a unique defense strategy where it expels blood from its eyes to deter predators. This defensive action can be modeled mathematically as projectile motion, with its trajectory described by the following equation:

$$\vec{x}_i(t+1)\& = \left[v_o \cos\left(\alpha \frac{t}{\text{Max\_iter}}\right) + \varepsilon\right]\vec{x}_{\text{best}}(t) \& + \left[v_o \sin\left(\alpha - \frac{\alpha t}{\text{Max\_iter}}\right) - g + \varepsilon\right]\vec{x}_i(t) \tag{36}$$

In the given model, $\vec{x}_i(t+1)$ represents the position of the new search agent (styled after the horned lizard) in the solution space for the subsequent generation, $t+1$. The optimal search agent from the current generation is $\vec{x}_{\text{best}}$, and $\vec{x}_i(t)$ denotes the current search agent's position. The variable *Max_iter* indicates the maximum allowable iterations, t represents the current iteration, v_o is initialized at 1 seg, α is set at $\pi/2$, ε is assigned a value of 1E-6, and g, representing Earth's gravitational acceleration, is taken as 0.009807 km/s^2.

4.4. Move-to-escape

The horned lizard employs a rapid and erratic movement strategy to evade predators. This behavior is mathematically modeled using a function that incorporates both local and global movements, as described in Eq. (37). The local movement is characterized by the function $walk\left(\frac{1}{2} - \varepsilon\right)$, which details the immediate area around the position $\vec{x}_i(t)$. Meanwhile, global movement is integrated by adding the position of the best search agent, $\vec{x}_{\text{best}}(t)$.

$$\vec{x}_i(t+1) = \vec{x}_{\text{best}}(t) + \text{walk}\left(\frac{1}{2} - \varepsilon\right)\vec{x}_i(t) \tag{37}$$

In the solution search space, $\vec{x}_i(t+1)$ represents the position of the new search agent, known as the horned lizard, for the next generation $t+1$. The current position for the i^{th} search agent at generation t is denoted by $\vec{x}_i(t)$. The best-performing agent in generation t is identified as $\vec{x}_{\text{best}}(t)$. A random number, *walk*, is generated between -1 and 1 to simulate movement, and ε is a random value drawn from a standard Cauchy distribution with both mean and θ parameters set to 0 and 1, respectively.

4.5. α -Melanophore stimulating hormone (α-MSH) rate

Horned lizards possess the capability to rapidly alter their skin color to adjust their solar thermal intake, a process influenced by temperature-dependent α -MSH. In this research, the rate of α -MSH in horned lizards

is quantified using Eq. (38). If the α -MSH rate falls below 0.3, it triggers the replacement of search agents as specified in Eq. (39). The vector of values, *melanophore*(i), derived from Eq. (38) is then normalized within the range [0,1].

$$\text{melanophore}\ (i) = \frac{\text{Fitness}_{\max} - \text{Fitness}\ (i)}{\text{Fitness}_{\max} - \text{Fitness}_{\min}} \tag{38}$$

$$\vec{x}_i(t) = \vec{x}_{\text{best}}\ (t) + \frac{1}{2}\left[\vec{x}_{r_1}(t) - (-1)^{\theta}\vec{x}_{r_2}(t)\right] \tag{39}$$

In the current generation t, $Fitness_{\min}$ and $Fitness_{\max}$ represent the best and worst fitness values, respectively. Meanwhile, $Fitness(i)$ refers to the fitness value of the i^{th}search agent at this stage.

The selection of the HLOA is justified due to its superior performance on benchmark tests and real-world applications. HLOA has demonstrated consistent high rankings in statistical tests like the Wilcoxon rank-sum and Friedman tests, outperforming other bio-inspired algorithms in various scenarios. It excels in handling complex optimization problems with unknown search spaces, requires minimal parameter configuration, and has proven effective in minimizing costs and enhancing performance in real-world engineering problems.

Fig. 4 shows the HLOA for the optimal operation solution.

5. Numerical results

The proposed method is tested on the IEEE 33-bus electric distribution system, as shown in Fig. 5. This system operates at a base voltage of 12.66 kV, with a nominal active load of 3715 kW and a nominal reactive load of 2300 kVAr, supported by a base of 100 MVA (Kashem et al., 2000). It is analyzed considering loads, prices, radiation, and temperature uncertainties, detailed in earlier sections. Meta-heuristic algorithms utilize random numbers and require multiple runs to produce reliable solutions. Therefore, the algorithm is executed several times for each of the three scenarios under study to ensure accurate comparisons. The maximum number of iterations is 100, and the population size is 30.

The optimal placement and sizing of PVs and D-STATCOMs, along with system reconfiguration, were determined using a computer equipped with an Intel Core i7–3537 processor, 6 GB RAM, and a 64-bit operating system. The analyses were conducted using MATLAB 2014a software.

The backward/forward sweep method was used for load flow analysis in the distribution systems. This method is favored for its computational accuracy, strong convergence properties, minimal memory usage, and straightforward application (Abou El-Ela et al., 2016).

In the case of an initial distribution network before reconfiguration, branch currents are calculated from network node currents and the [BIBC] matrix (Teng, 2003).

$$[I] = [BIBC][I_L] \tag{40}$$

The distribution network reconfiguration uses the reconfigured BIBC matrix, denoted [*rBIBC*], and the branch current expressions are calculated as follows (Şeker et al., 2021).

$$[rI] = [rBIBC][I_L] \tag{41}$$

The studied distribution network consists of 5 additional lines, thus forming 5 loops. The reconfiguration procedure consists of opening only one line among those constituting each loop. This operation must comply with the following points:

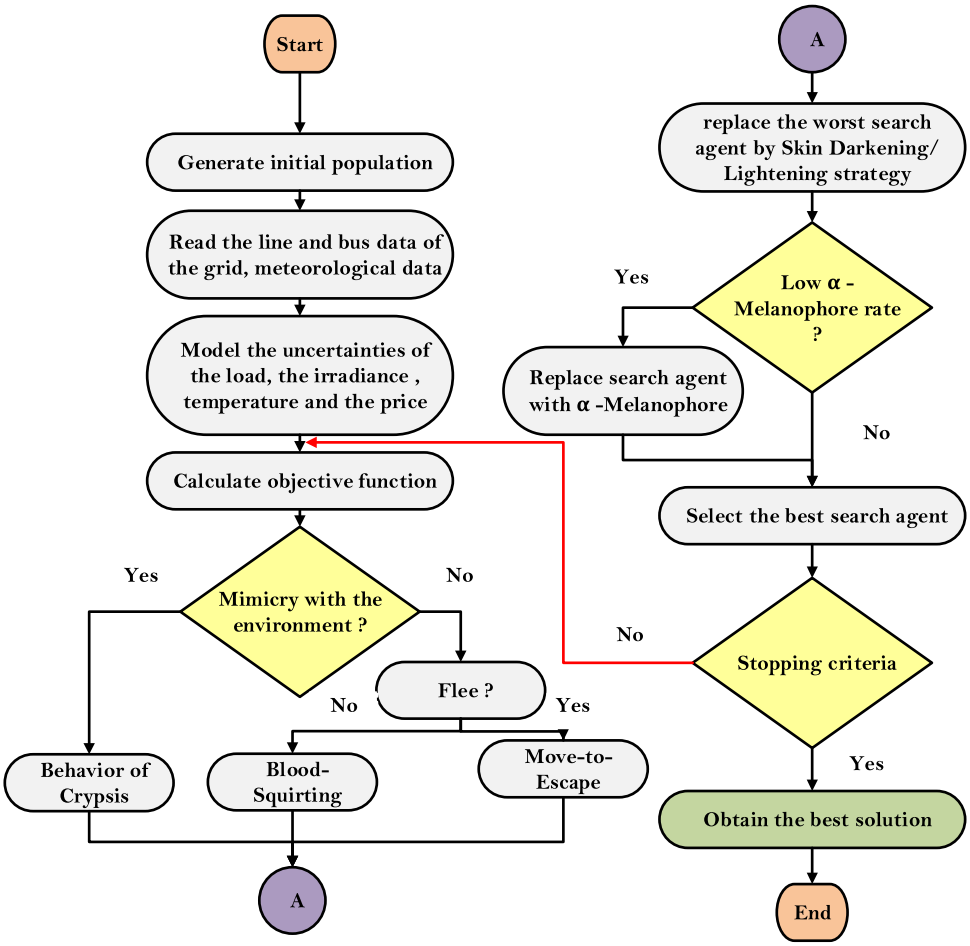

Fig. 4. Flowchart illustrating the most optimal operational solution for the proposed HLOA.

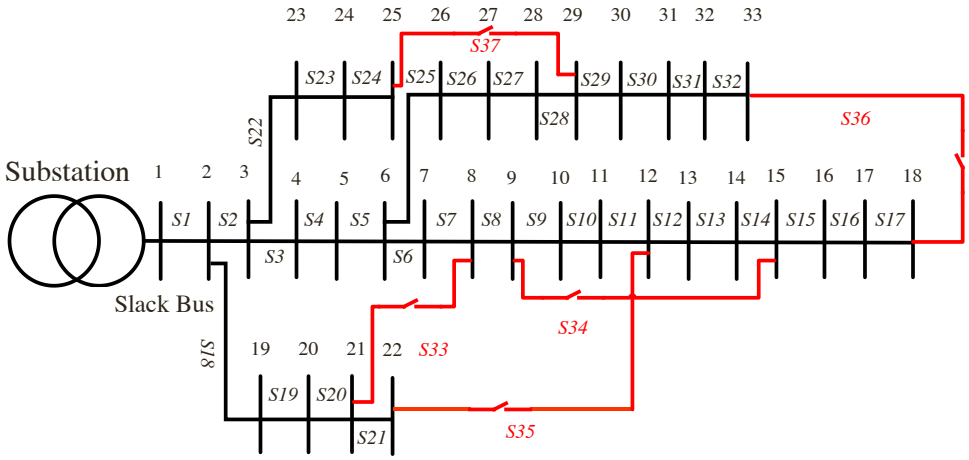

Fig. 5. The structure of the IEEE 33-bus distribution system topology.

– The distribution network after reconfiguration must have a radial topology. (Constraint of radial configuration)
– Do not open the same line on several loops.
– Ensure that all loads are supplied (constraints of isolation)

The following scenarios have been taken into account while evaluating the system performance:

- ***Scenario #1***: The base case, before adding PVs and D-STATCOMs, and without reconfiguration.
- ***Scenario #2***: Integration of PV systems only, without incorporating D-STATCOMs or utilizing reconfiguration.
- ***Scenario #3***: Combining PVs and D-STATCOMs together in a single system without employing reconfiguration.
- ***Scenario #4***: Integrating PVs and D-STATCOMs with the implementation of reconfiguration.

Figs. 6 and 7 briefly depict the estimated temperature and solar irradiation alongside the anticipated market price and grid loading.

Various parameters were evaluated across each scenario to assess the effectiveness of different scenarios in optimizing the electrical distribution network. The table below outlines the optimal results achieved under different scenarios, including the location and size of PV units, the size of D-STATCOMs, the activation of open switches, as well as key performance indicators such as power losses, voltage deviation, total annual cost, total annual emissions, and the best MOF score. These results provide valuable insights into the impact of each scenario on network performance and overall efficiency. Table 3

The primary goal of this study was to minimize costs, reduce environmentally harmful emissions, and enhance the system's efficiency by integrating renewable energy sources and D-STATCOMs with network reconfiguration into an electrical distribution network. The results showed that the implementation of the HLOA algorithm led us to

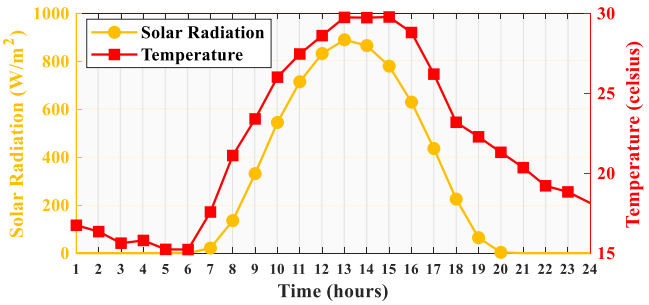

Fig. 6. The expected temperature and solar irradiation.

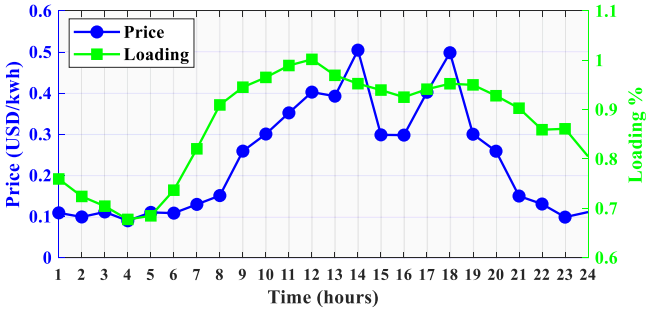

Fig. 7. The expected price and loading.

Table 3
Optimal results Across Various Scenarios.

Item	Scenario #1	Scenario #2	Scenario #3	Scenario #4
Optimal location	-	8 16 30	17 26 30	9 29 30
Optimal size of PV (kW)	-	2147.6 744.855 2061.2	305.235 1833 2818	2291.9 503.88 2121.1
Optimal size of D-STATCOMs (kVar)	-	- - -	209.363 822.202 422.395	702.42 282.457 524.694
Open switches	-	-	-	6, 13, 10, 36, 28
Power losses (kW)	3829.4e+03	2.7499e+03	1.7516e+03	1.2905e+03
Voltage deviation (p.u)	37.3592	23.8809	17.3312	10.8138
Total annual cost (USD/kWh)	7.4969e+06	4.2102e+06	4.1059e+06	4.0780e+06
Total annual emission (kg)	2.7579e+07	1.7874e+07	1.7530e+07	1.7450e+07
Best MOF	1	0.6418	0.5262	0.4508

discover the most effective solution to our optimization problem, resulting in reduced costs, voltage deviations, real power losses, and emissions.

No interventions were made in Scenario #1, which served as the base case, leading to the distribution network facing its highest operational challenges. In this scenario, power losses reached 3829.4 kW, and significant voltage deviations of 37.3592 per unit (P.U) were recorded. This resulted in a total annual cost of 7.4969e+06 USD and emissions totaling 2.7579e+07 kg.

In Scenario #2, only PV systems were integrated at optimal locations

on buses 8, 16, and 30, with capacities of 2147.6 kW, 744.855 kW, and 2061.2 kW. This intervention led to notable improvements in the network; power losses were significantly reduced to 2.7499e+03 kW, and voltage deviations dropped to 23.8809 p.u. Consequently, this resulted in a reduced annual cost of 4.2102e+06 USD and a lower emission level of 1.7874e+07 kg.

Building on the improvements seen in Scenario #2, Scenario #3 combined both PV systems and D-STATCOMs at buses 17, 26, and 30, with respective PV capacities of 305.235 kW, 1833 kW, and 2818 kW, and D-STATCOMs added at 209.363 kVar, 822.202 kVar, and 422.395 kVar. This hybrid system enhanced network stability by reducing power losses to 1.7516e+03 kW and minimizing voltage deviations to 17.3312 p.u. The enhancements in this scenario slightly reduced the total annual costs to 4.1059e+06 USD, with emissions at 1.7530e+07 kg.

Finally, Scenario #4 represented the most integrated approach, incorporating PV systems, D-STATCOMs, and comprehensive network reconfiguration. The optimal locations were at buses 9, 29, and 30, with PV units producing 2291.9 kW, 503.88 kW, and 2121.1 kW, and D-STATCOM units at 702.42 kVar, 282.457 kVar, and 524.694 kVar, alongside opening switches at 6, 13, 10, 36, and 28. This strategic adjustment led to the most optimized results, with the lowest power losses at 1.2905e+03 kW and minimal voltage deviations at 10.8138 p.u., achieving the lowest annual cost of approximately 4.0780e+06 USD and emissions reduced to 1.7450e+07 kg. This complete integration significantly enhanced network operations, delivering the best performance regarding cost-effectiveness, stability, and environmental impact, showcasing the profound benefits of a thoroughly optimized and reconfigured network system.

Fig. 8 provides a detailed hourly comparison across different scenarios, demonstrating that Scenario #4, which integrates PV systems, D-STATCOMs, and network reconfiguration, consistently yields the lowest values in power losses, voltage deviation, operational costs, and emissions. This scenario significantly enhances electrical network efficiency, as evidenced by its reduced power losses and voltage deviations. These reductions not only lead to substantial cost savings but also minimize environmental impacts by lowering emissions. The integration of renewable energy with D-STATCOMs and strategic network reconfiguration in Scenario #4 clearly results in the most beneficial outcomes compared to the other scenarios, showcasing its superiority in improving system performance and sustainability.

In examining the effectiveness of various enhancements to an electrical distribution system, Fig. 9 presents a clear comparative analysis of the voltage profiles across four scenarios. From this comparison, it is evident that Scenario #4 achieves the best voltage profile compared to the others. This indicates that the combination of PV systems, D-STATCOMs, and network reconfiguration in Scenario #4 provides the most stable voltage levels across the network.

Table 4 and Fig. 10 present the algorithmic results and convergence curves for the various scenarios using different optimization techniques: Reptile Search Algorithm (RSA) (Abualigah et al., 2022), Sine Cosine Algorithm (SCA) (Mirjalili, 2016), Beluga Whale Optimization (BWO) (Zhong et al., 2022), and Horned Lizard Optimization Algorithm (HLOA).

Table 4 shows that HLOA consistently outperforms the other algorithms in terms of average, best, and worst performance metrics across all scenarios. Specifically, HLOA achieves the lowest average, best, and worst scores in each scenario, underscoring its efficiency and robustness in optimizing under varied conditions. This superiority is visually

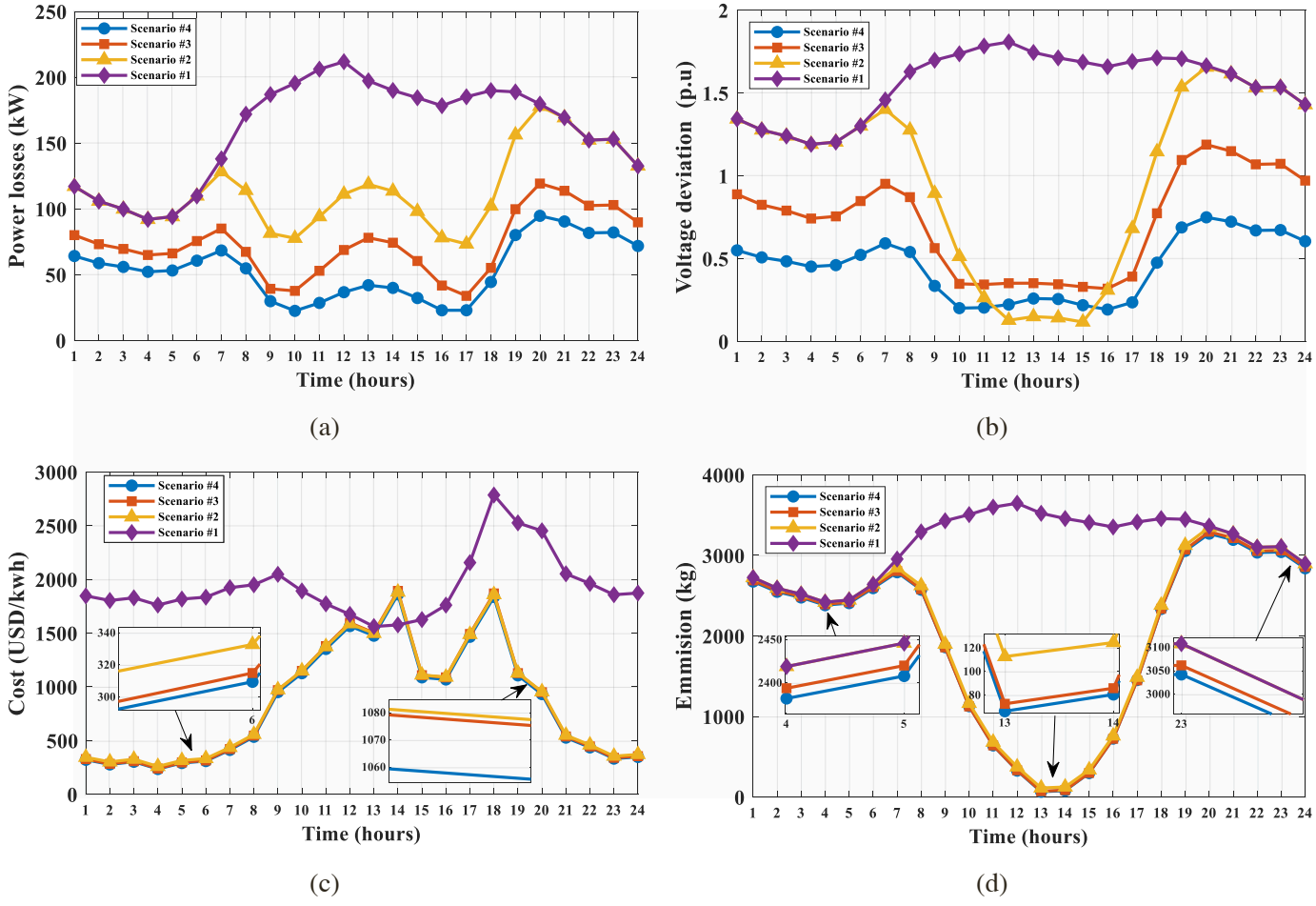

Fig. 8. Hourly results across different scenarios for: (a) Power losses, (b) Voltage deviation, (c) Cost, (d) Emission.

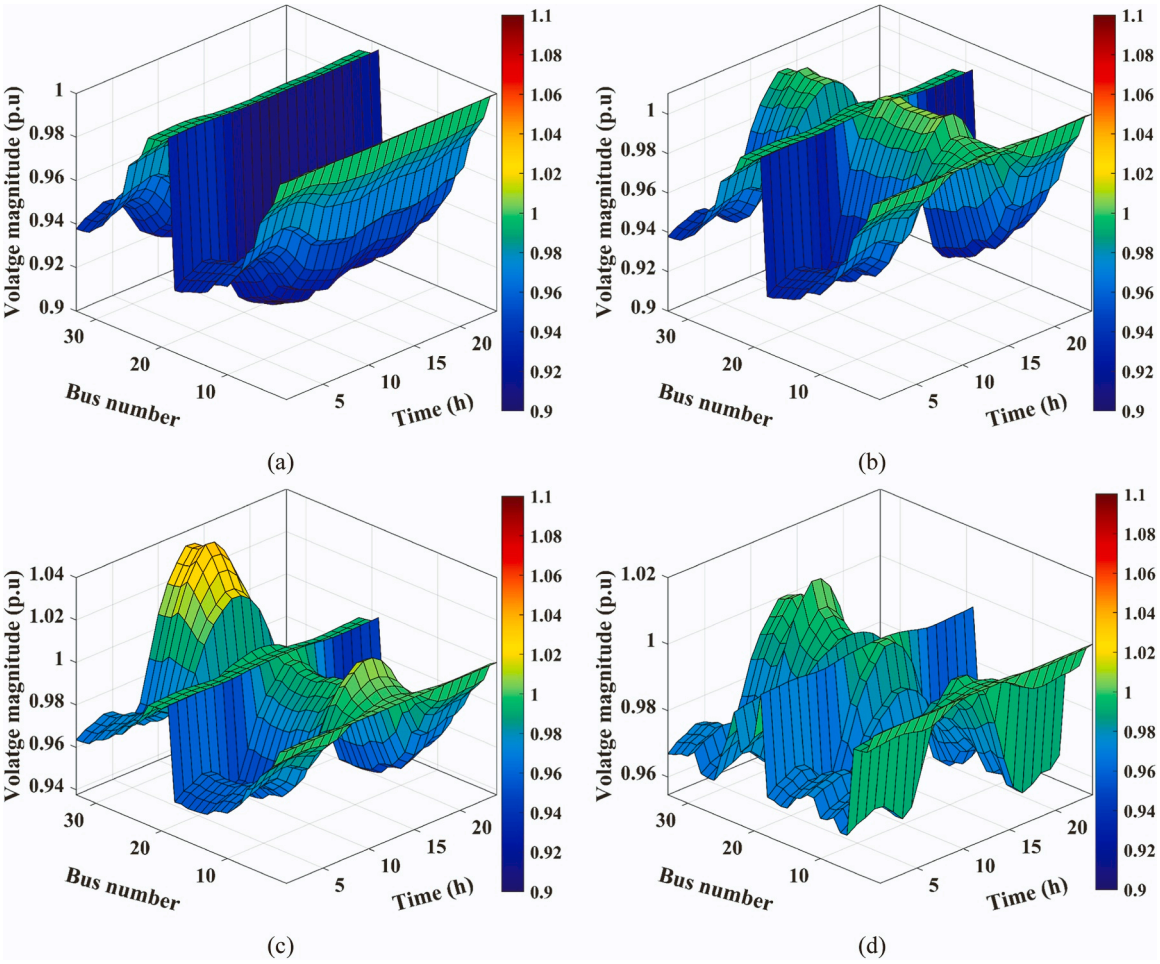

Fig. 9. Voltage profiles results for: (a) Scenario #1, (b) Scenario #2, (c) Scenario #3, (d) Scenario #4.

Table 4
Algorithmic Results Across Various Scenarios.

Algorithm	Scenario #2			Scenario #3			Scenario #4		
	Average	Best	Worst	Average	Best	Worst	Average	Best	Worst
RSA	0.6798	0.6554	0.7169	0.7414	0.5989	0.8588	0.6890	0.5831	0.7695
SCA	0.6568	0.6525	0.6596	0.5640	0.5540	0.5835	0.6371	0.5827	0.7367
BWO	0.6597	0.6539	0.6675	0.6038	0.5817	0.6218	0.5997	0.5857	0.6190
HLOA	0.6481	0.6418	0.6563	0.5511	0.5262	0.5644	0.4538	0.4508	0.4592

confirmed in Fig. 10, where the convergence curves for HLOA reach lower values more quickly than those for RSA, SCA, and BWO, indicating a faster and more effective optimization process.

6. Conclusions

In this paper, the key performance indicators, including Total Real Power Losses (TRPL), Total Operation Cost, Total Voltage Deviation (TVD), and Total Emission (TE), have been investigated under the optimal integration of photovoltaic (PV) systems and Distribution Static Compensators (D-STATCOMs) through the determination of both the optimal placement and sizing of PV units and D-STATCOMs simultaneously, as well as the implementation of network reconfiguration based on the Horned Lizard Optimization Algorithm (HLOA) technique. The investigation was carried out under the uncertainties of solar irradiation, temperature, load demand, and electricity pricing, in which the Monte Carlo Simulation (MCS) based on the Probability Density Functions (PDFs) along with the Scenario Reduction Algorithm (SRA) has been used for addressing the uncertainty of the system. The efficiency of the proposed HLOA method is demonstrated on the IEEE 33-bus distribution system. The key findings of this research are that substantial improvements in system performance, cost-effectiveness, and environmental sustainability can be attained with the appropriate integration of PV systems, D-STATCOMs, and network reconfiguration, in which the overall cost is reduced by 45.6 %, real power losses are decreased by 66.3 %, voltage variations are improved by 71.04 %. Emissions are

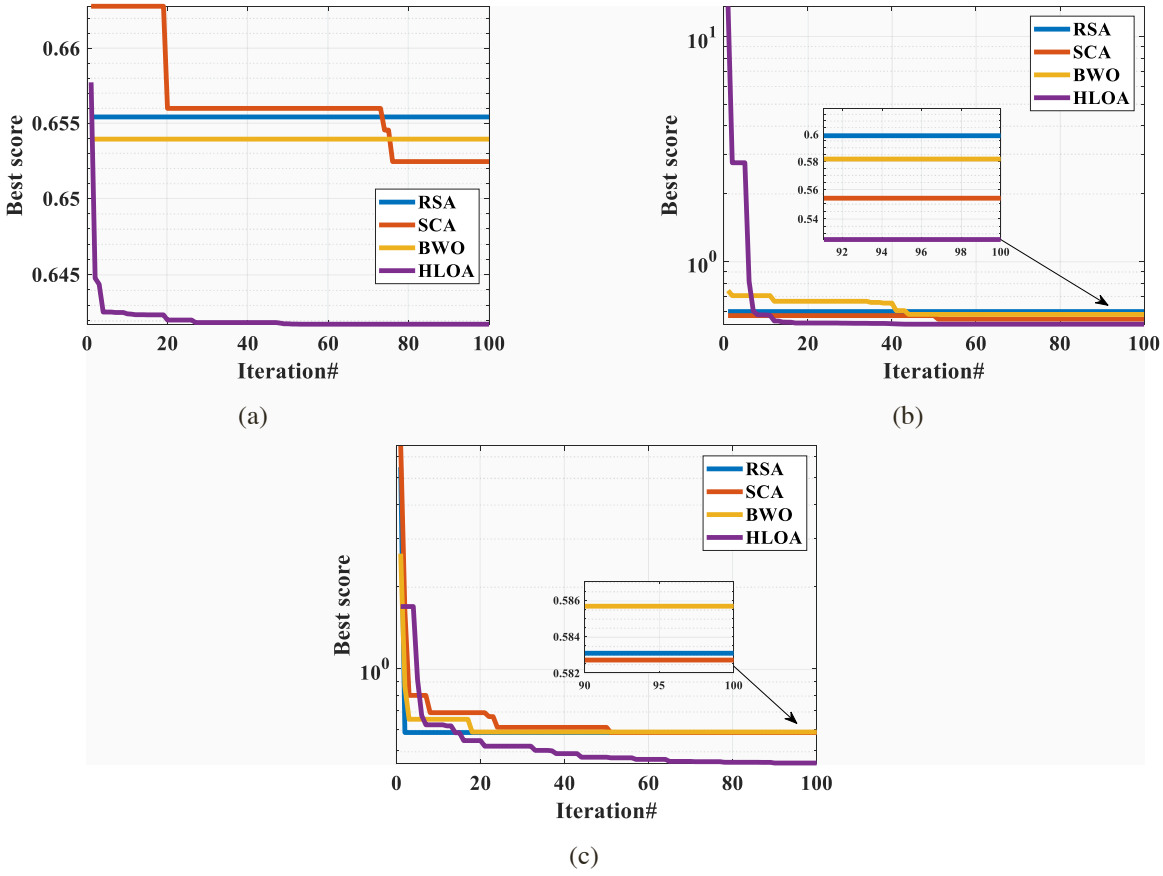

Fig. 10. Convergence curve results for: (a) Scenario #2, (b) Scenario #3, (c) Scenario #4.

mitigated by 36.72 %, compared to the base case scenario without integration or reconfiguration. However, several limitations must be acknowledged. The study does not address the integration of storage systems into the grid to store excess energy produced by PV systems, which is essential for optimizing renewable energy utilization. Additionally, demand response strategies, which can significantly enhance grid stability and efficiency, were not explored.

CRediT authorship contribution statement

Ahmed Hachemi: Writing – original draft, Visualization, Validation, Software, Resources, Methodology, Investigation, Formal analysis, Data curation, Conceptualization. **Fares Sadaoui:** Writing – review & editing, Validation, Supervision, Software, Methodology, Investigation, Data curation, Conceptualization. **Abdelhakim Saim:** Writing – review & editing, Supervision, Software, Resources, Funding acquisition, Data curation, Conceptualization. **Mohamed Ebeed:** Writing – review & editing, Validation, Supervision, Software, Formal analysis. **Salem Arif:** Writing – review & editing, Supervision, Resources, Project administration, Conceptualization.

Declaration of Competing Interest

The authors declare that they have no known competing financial interests or personal relationships that could have appeared to influence the work reported in this paper. The authors declare the following financial interests/personal relationships which may be considered as potential competing interests: none.

Data Availability

Data will be made available on request.

Acknowledgments

This research was partially supported by the National Research Agency (ANR), LEAP RE “MiDiNA—Microgrids Development in North Africa” project, grant number “ANR-23-LERE-0002–01”.

References

Abbas, G., Wu, Z., Ali, A., 2024. Multi-objective multi-period optimal site and size of distributed generation along with network reconfiguration. IET Renew. Power Gener.

Abou El-Ela, A.A., El-Sehiemy, R.A., Kinawy, A.M., Mouwafi, M.T., 2016. Optimal capacitor placement in distribution systems for power loss reduction and voltage profile improvement. IET Gener. Transm. Distrib. vol. 10 (5), 1209–1221.

Abualigah, L., Abd Elaziz, M., Sumari, P., Geem, Z.W., Gandomi, A.H., 2022. Reptile search algorithm (RSA): a nature-inspired meta-heuristic optimizer,". Expert Syst. Appl. vol. 191, 116158.

Ahmed, D., et al., 2024. An enhanced jellyfish search optimizer for stochastic energy management of multi-microgrids with wind turbines, biomass and PV generation systems considering uncertainty. Sci. Rep. vol. 14.

Akbari, M.A., et al., 2017. New metrics for evaluating technical benefits and risks of DGs increasing penetration. IEEE Trans. Smart Grid vol. 8 (6), 2890–2902.

Amigue, F.F., Essiane, S.N., Ngoffe, S.P., Ondoa, G.A., Mengounou, G.M., Nna, P.N., 2021. Optimal integration of photovoltaic power into the electricity network using Slime mould algorithms: application to the interconnected grid in North Cameroon. Energy Rep. vol. 7, 6292–6307.

Asaad, A., et al., 2023. Multi-objective optimal planning of EV charging stations and renewable energy resources for smart microgrids. Energy Sci. Eng. vol. 11 (3), 1202–1218.

Augustine, N., Suresh, S., Moghe, P., Sheikh, K., 2012. Economic Dispatch for A Microgrid Considering Renewable Energy Cost Functions. 2012 IEEE PES Innovative Smart Grid Technologies *(ISGT)*. IEEE, pp. 1–7.

T.U. Badrudeen, F.K. Ariyo, and N. Nwulu, Voltage stability improvement and power losses reduction through multiple grid contingency supports, Energy Exploration & Exploitation, p. 01445987231218292, 2024.
Bahrami, S., Chen, Y.C., Wong, V.W., 2024. Dynamic distribution network reconfiguration with generation and load uncertainty. IEEE Trans. Smart Grid.
Balu, K., Mukherjee, V., 2024. Optimal deployment of electric vehicle charging stations, renewable distributed generation with battery energy storage and distribution static compensator in radial distribution network considering uncertainties of load and generation. Appl. Energy vol. 359, 122707.
Biswas, P.P., Suganthan, P.N., Mallipeddi, R., Amaratunga, G.A., 2019. Optimal reactive power dispatch with uncertainties in load demand and renewable energy sources adopting scenario-based approach. Appl. Soft Comput. vol. 75, 616–632.
Diaf, S., Diaf, D., Belhamel, M., Haddadi, M., Louche, A., 2007. A methodology for optimal sizing of autonomous hybrid PV/wind system. Energy Policy vol. 35 (11), 5708–5718.
Ebeed, M., et al., 2024a. Optimal integrating inverter-based PVs with inherent DSTATCOM functionality for reliability and security improvement at seasonal uncertainty. Sol. Energy vol. 267, 112200.
Ebeed, M., et al., 2024b. "Solving stochastic optimal reactive power dispatch using an adaptive Beluga Whale optimization considering uncertainties of renewable energy resources and the load growth,". Ain Shams Eng. J., 102762
Ebeed, M., Ali, A., Mosaad, M.I., Kamel, S., 2020. An improved lightning attachment procedure optimizer for optimal reactive power dispatch with uncertainty in renewable energy resources. IEEE Access vol. 8, 168721–168731.
Elseify, M.A., Hashim, F.A., Hussien, A.G., Abdel-Mawgoud, H., Kamel, S., 2024. Boosting prairie dog optimizer for optimal planning of multiple wind turbine and photovoltaic distributed generators in distribution networks considering different dynamic load models. Sci. Rep. vol. 14 (1), 1–33.
Emrani, A., Berrada, A., 2024. A comprehensive review on techno-economic assessment of hybrid energy storage systems integrated with renewable energy. J. Energy Storage vol. 84, 111010.
Esmaeili, M., Sedighizadeh, M., Esmaili, M., 2016. Multi-objective optimal reconfiguration and DG (Distributed Generation) power allocation in distribution networks using Big Bang-Big Crunch algorithm considering load uncertainty. Energy vol. 103, 86–99.
Gampa, S.R., Das, D., 2015. Optimum placement and sizing of DGs considering average hourly variations of load. Int. J. Electr. Power Energy Syst. vol. 66, 25–40.
Gil-González, W., 2023. Optimal placement and sizing of d-statcoms in electrical distribution networks using a stochastic mixed-integer convex model. Electronics vol. 12 (7), 1565.
N. Growe-Kuska, H. Heitsch, and W. Romisch, Scenario Reduction and Scenario Tree Construction for Power Management Problems, in 2003 IEEE Bologna Power Tech Conference Proceedings, 2003, vol. 3: IEEE, p. 7 pp. Vol. 3.
Hachemi, A.T., et al., 2023a. Modified reptile search algorithm for optimal integration of renewable energy sources in distribution networks. Energy Sci. Eng. vol. 11 (12), 4635–4665.
A. Hachemi, F. Sadaoui, and S. Arif, Optimal Location and Sizing of Capacitor Banks in Distribution Systems Using Grey Wolf Optimization Algorithm, in International Conference on Artificial Intelligence in Renewable Energetic Systems, 2022: Springer, pp. 719-728.
Hachemi, A.T., Sadaoui, F., Saim, A., Ebeed, M., Abbou, H.E., Arif, S., 2023b. Optimal operation of distribution networks considering renewable energy sources integration and demand side response. Sustainability vol. 15 (24), 16707.
Hasanien, H.M., Alsaleh, I., Ullah, Z., Alassaf, A., 2024. Probabilistic optimal power flow in power systems with renewable energy integration using enhanced walrus optimization algorithm. Ain Shams Eng. J. vol. 15 (3), 102663.
Hassan, Q., , 2024. The renewable energy role in the global energy transformations. Renewable Energy Focus vol. 48, 100545.
Kamel, R.M., Hashem, M., Ebeed, M., Ali, A., 2024. Enhancing the reliability and security of distribution networks with plug-in electric vehicles and wind turbine generators considering their stochastic natures. Sustain. Energy Grids Netw., 101439
Kanase, D.B., Jadhav, H., 2024. Solar PV system and battery-operated DSTATCOM for power quality enhancement: a review. MAPAN 1–23.
Kashem, M., Ganapathy, V., Jasmon, G., Buhari, M., 2000. A novel method for loss minimization in distribution networks," in DRPT2000. International conference on electric utility deregulation and restructuring and power technologies. Proceedings (Cat. No. 00EX382), 2000: IEEE, pp. 251-256. 251–256 ((IEEE)).
Khalid, M., 2024. Smart grids and renewable energy systems: perspectives and grid integration challenges. Energy Strategy Rev. vol. 51, 101299.
Kilic, H., Asker, M.E., Haydaroglu, C., 2024. Enhancing power system reliability: hydrogen fuel cell-integrated D-STATCOM for voltage sag mitigation. Int. J. Hydrog. Energy.
Li, L.-L., Fan, X.-D., Wu, K.-J., Sethanan, K., Tseng, M.-L., 2024. Multi-objective distributed generation hierarchical optimal planning in distribution network: improved beluga whale optimization algorithm. Expert Syst. Appl. vol. 237, 121406.
Liao, X., Zhou, Z., Li, Z., Huai, Q., 2023. Dynamic reconfiguration of AC/DC hybrid distribution network considering non-ideal linear BES model. Energy Rep. vol. 9, 5628–5646.
Liu, S., et al., 2024. Integration method of large-scale photovoltaic system in distribution network based on improved multi-objective TLBO algorithm. Front. Energy Res. vol. 11, 1322111.
Mahdavi, M., Javadi, M.S., Wang, F., Catalão, J.P., 2022. An efficient model for accurate evaluation of consumption pattern in distribution system reconfiguration. IEEE Trans. Ind. Appl. vol. 58 (3), 3102–3111.
Marquez, J.A., et al., 2023. Optimal planning and operation of distribution systems using network reconfiguration and flexibility services. Energy Rep. vol. 9, 3910–3919.
Mirjalili, S., 2016. SCA: a sine cosine algorithm for solving optimization problems. Knowl. Based Syst. vol. 96, 120–133.
Mohamed, M.A.-E.-H., Kamel, S., Alrashed, M.M., Elnaggar, M.F., 2024. Power flow optimization in distribution networks: estimating optimal distribution generators through pseudo-inverse analysis. Energy Rep. vol. 11, 2935–2970.
Montoya, O.D., Ramírez-Vanegas, C.A., González-Granada, J.R., 2024. Dynamic active and reactive power compensation in distribution networks using PV-STATCOMs: a tutorial using the Julia Software. Results Eng., 101876
Morstyn, T., Teytelboym, A., Hepburn, C., McCulloch, M.D., 2019. Integrating P2P energy trading with probabilistic distribution locational marginal pricing. IEEE Trans. Smart Grid vol. 11 (4), 3095–3106.
Noruzi Azghandi, M., Shojaei, A.A., Toosi, S., Lotfi, H., 2023. Optimal reconfiguration of distribution network feeders considering electrical vehicles and distributed generators. Evolut. Intell. vol. 16 (1), 49–66.
Oda, E.S., Abd El Hamed, A.M., Ali, A., Elbaset, A.A., Abd, M., Sattar, El, Ebeed, M, 2021. Stochastic optimal planning of distribution system considering integrated photovoltaic-based DG and DSTATCOM under uncertainties of loads and solar irradiance. IEEE Access vol. 9, 26541–26555.
Ortega-Romero, I., Serrano-Guerrero, X., Barragán-Escandón, A., Ochoa-Malhaber, C., 2023. Optimal integration of distributed generation in long medium-voltage electrical networks. Energy Rep. vol. 10, 2865–2879.
Pan, J.-S., Wang, H.-J., Nguyen, T.-T., Zou, F.-M., Chu, S.-C., 2022. Dynamic reconfiguration of distribution network based on dynamic optimal period division and multi-group flight slime mould algorithm. Electr. Power Syst. Res. vol. 208, 107925.
Peraza-Vázquez, H., Peña-Delgado, A., Merino-Treviño, M., Morales-Cepeda, A.B., Sinha, N., 2024. A novel metaheuristic inspired by horned lizard defense tactics. Artif. Intell. Rev. vol. 57 (3), 59.
Piri, A., Aghanajafi, C., Sohani, A., 2023. Enhancing efficiency of a renewable energy assisted system with adiabatic compressed-air energy storage by application of multiple Kalina recovery cycles. J. Energy Storage vol. 61, 106712.
Purlu, M., Turkay, B.E., 2022. Optimal allocation of renewable distributed generations using heuristic methods to minimize annual energy losses and voltage deviation index. IEEE Access vol. 10, 21455–21474.
Ramadan, A., Ebeed, M., Kamel, S., Agwa, A.M., Tostado-Véliz, M., 2022. The probabilistic optimal integration of renewable distributed generators considering the time-varying load based on an artificial gorilla troops optimizer. Energies vol. 15 (4), 1302.
Rincón-Miranda, A., Gantiva-Mora, G.V., Montoya, O.D., 2023. Simultaneous integration of D-STATCOMs and PV Sources in distribution networks to reduce annual investment and operating costs. Computation vol. 11 (7), 145.
R.Y. Rubinstein and D. Kroese, Simulation and the Monte Carlo Method. john wiley&sons," *Inc. Publication,* 1981.
Şeker, A.A., Gözel, T., Hocaoğlu, M.H., 2021. BIBC matrix modification for network topology changes: reconfiguration problem implementation. Energies vol. 14 (10), 2738.
Shojaabadi, S., Abapour, S., Abapour, M., Nahavandi, A., 2016. Simultaneous planning of plug-in hybrid electric vehicle charging stations and wind power generation in distribution networks considering uncertainties. Renew. Energy vol. 99, 237–252.
Sultana, S., Roy, P.K., 2014. Optimal capacitor placement in radial distribution systems using teaching learning based optimization. Int. J. Electr. Power Energy Syst. vol. 54, 387–398.
Tatikayala, V.K., Dixit, S., 2024. Multi-stage voltage control in high photovoltaic based distributed generation penetrated distribution system considering smart inverter reactive power capability. Ain Shams Eng. J. vol. 15 (1), 102265.
Teng, J.-H., 2003. A direct approach for distribution system load flow solutions. IEEE Trans. Power Deliv. vol. 18 (3), 882–887.
Wang, X., Liu, X., Jian, S., Peng, X., Yuan, H., 2021. A distribution network reconfiguration method based on comprehensive analysis of operation scenarios in the long-term time period. Energy Rep. vol. 7, 369–379.
Woldesemayat, M.L., Biramo, D.B., Tantu, A.T., 2024. Assessment of power distribution system losses and mitigation through optimally placed D-STATCOM. Cogent Eng. vol. 11 (1), 2330824.
Yuvaraj, T., Suresh, T., Meyyappan, U., Aljafari, B., Thanikanti, S.B., 2023. Optimizing the allocation of renewable DGs, DSTATCOM, and BESS to mitigate the impact of electric vehicle charging stations on radial distribution systems. Heliyon vol. 9 (12).
Zhong, C., Li, G., Meng, Z., 2022. Beluga whale optimization: a novel nature-inspired metaheuristic algorithm,". Knowl. Based Syst. vol. 251, 109215.
Zubo, R.H., Mokryani, G., Abd-Alhameed, R., 2018. Optimal operation of distribution networks with high penetration of wind and solar power within a joint active and reactive distribution market environment. Appl. Energy vol. 220, 713–722.